European Review for Medical and Pharmacological Sciences 2021; 25: 2927-2940

# Identification of hub prognosis-associated oxidative stress genes in skin cutaneous melanoma using integrated bioinformatic analysis

T.-Y. REN[1], Y.-X. ZHANG[2], W. HU[1]

[1]Department of Spine and Joint Surgery, Guilin Peoples' Hospital, Guilin, China
[2]Department of Anesthesia, Guilin Peoples' Hospital, Guilin, China

*Tianyu Ren and Yuxuan Zhang contributed equally to this manuscript*

**Abstract. – OBJECTIVE: Oxidative stress (OS) significantly correlates with cancer progression. However, targeting OS has not been considered as a therapeutic strategy in skin cutaneous melanoma (SKCM) due to a lack of systematical studies on validated biomarkers. The work presented here aimed to identify hub prognosis-associated OS genes in SKCM and generated an effective predictive model.**

**PATIENTS AND METHODS: Gene expression profiles of SKCM samples and normal skin tissues were obtained from the Genotype-Tissue Expression (GTEx) and The Cancer Genome Atlas (TCGA) databases to identify differentially expressed OS genes. The validation cohort was obtained from the Gene Expression Omnibus (GEO) database.**

**RESULTS: Thirteen hub prognosis-associated OS genes were recognized and incorporated into the prognostic risk model. Our constructed model was significantly associated with overall survival of SKCM patients as well as was shown to be associated with cancer progression. Our prognostic risk model was found to improve the accuracy of diagnostics, as shown using both TCGA and GEO cohorts. Both hub gene expression and risk score were used to generated nomograms that displayed favorable discriminatory abilities for SKCM.**

**CONCLUSIONS: Overall, our study presents a model that may provide novel insights into the prognosis and survival of SKCM patients, as well as the development of individualized treatment therapy.**

*Key Words:*
Integrated bioinformatic analysis, Oxidative stress, Prognosis, Skin cutaneous melanoma.

## Introduction

Skin cutaneous melanoma (SKCM) is an aggressive malignant tumor that poses a serious threat to health[1]. In 2018, 287,723 new patients were diagnosed with melanoma around the world and 21.1% of these patients passed away from the disease[2]. Metastatic SKCM results in the greater number of deaths related to skin tumors[3]. Patients diagnosed with SKCM in stages I and II have a 10-year overall survival rate of 75 to 98%[4]. However, one-third of these patients develop metastatic melanoma. In contrast, for SKCM patients diagnosed in stages IIIA to IIID, the 10-year overall survival rate is decreased and ranges between 24-88%. These data suggest that early diagnosis of SKCM is essential for a favorable outcome[5]. Even though some theories indicate that tumorigenesis and progression are related to skin pigmentation[6,7] and that pathogenesis is associated with acquired melanocytic nevi, family history and genetic susceptibility[8,9], but this pathogenesis behind SKCM is still not known. Accurate diagnosis of SKCM at early stages is the main objective. Some work is focusing on uncovering new biomarkers related to the prediction of progression and prognosis of SKCM that can also be used for personalized treatment[10,11]. However, only a few clinically relevant biomarkers and tools for SKCM are available[12]. It is thus necessary to uncover additional biomarkers potentially able to aid in the diagnosis and identifying the prognosis behind SKCM cases.

Oxidative stress (OS) is the result of an imbalance of oxidants and antioxidants and promotes increased levels of reactive oxygen species (ROS). ROS includes singlet oxygens, hydrogen peroxide and superoxide anion[13]. The overproduction of ROS is observed in patients with SKCM and suggests that ROS may drive cancer development and progression[14-17]. The presence of excessive ROS leads to DNA damage and genotoxicity[18,19] and increases the chances of mutations that can

*Corresponding Author:* Wei Hu, MD: e-mail: huweidoctor@163.com

lead to cancer[20,21]. In skin cells, ROS are generated by the NADPH oxidase family of enzymes, nitric oxide synthase, arachidonic acid oxygenase activities and mitochondria primarily in melanosomes[22]. Even though melanin has protective effects on melanocytes when it comes to protecting cells against UV radiation, synthesis of melanin can also be harmful since it is associated with increased levels of intracellular ROS[23,24].

Bioinformatics has been used to identify disease-specific biomarkers for SKCM[25,26]. However, differentially expressed genes are identified from a single analysis method which lacks discriminatory ability for highly connected genes. Meanwhile, sole focus on the expression levels of individual genes ignores intergenomic epistasis. Weighted gene co-expression network (WGCN) is used to evaluate the association between genes and phenotypic traits rather than focusing on individual gene expression[27]. During WGCN analysis (WGCNA), SKCM expression data can be used to identify hub biomarkers for diagnosis and prognosis[28,29]. Furthermore, differential gene expression analysis of transcriptional data is another powerful tool providing changes in quantitative expression levels between two subgroups[30]. In this study, candidate OS genes differentially expressed in SKCM tissues *vs.* normal skin were identified using WGCNA and differential gene expression analysis to enhance the discriminatory ability of highly connected genes. Subsequently, univariate Cox regression and least absolute shrinkage and selection operator (LASSO) analyses were also used to identify hub genes significantly related to SKCM prognosis. A prognostic risk model was generated based on hub gene expression. The significance of each gene was explored in SKCM patients. To date, most prognostic risk models for SKCM were mainly constructed based on tumor immunity[31], miRNAs and lncRNA signatures[32,33]. However, these studies used simplified univariate analysis[34] and none systemically explored OS genes in SKCM and their prognostic value. Thus, the study presented here uncovers the first OS-associated risk model that can provide novel insight into diagnosis and prognosis of SKCM cases.

## Patients and Methods

### Patients

Both RNA-sequencing data and clinical information for the 471 SKCM and 1 normal skin tissue samples were obtained from the University of California Santa Cruz Xena (UCSC Xena; http://xena.ucsc.edu/)[35]. The Genotype-Tissue Expression (GTEx) database (https://gtexportal.org/home/datasets) was used to obtain transcriptome data for 812 normal skin samples[36,37]. In addition, the Gene Expression Omnibus (GEO) GSE65904 cohort (https://www.ncbi.nlm.nih.gov/geo/), which contained gene expression profiles and clinical data for a total of 214 SKCM patients, was used as a validation cohort[38]. R software and specific packages were used to perform bioinformatic analyses. Log2-transformation and normalization using the "sva" package were performed to remove batch effects[39,40]. To obtain OS-associated genes, GeneCards database (https://www.genecards.org) was used to obtain 1399 protein domains for the specific OS genes with a relevance score $\geq 7$.

### WGCN Construction and the Identification of the Hub Module

A gene co-expression networking using the "WGCNA" package[41] was generated using OS gene expression profiles for SKCM cases in the TCGA. Pairwise Pearson's correlation coefficients were determined between all the genes. The following formula was used to identify a weighted adjacency matrix: amn=|cmn|β (cmn = Pearson's correlation between gene m and gene n; amn = adjacency between gene m and gene n). Next, a parameter for "β" was identified to choose strong gene correlations. A topological overlap matrix (TOM) transformed adjacencies. Average linkage hierarchical clustering was used to construct OS gene dendrograms with a minimum module size of 50. Dissimilarities of module eigengenes were calculated. Furthermore, module eigengenes and gene significance revealed modules relevant to SKCM clinical traits. Genes in the functional module were labeled as candidates.

### Differential Expression Analysis and Interactions

Differential expression analysis using the "limma" package compared SKCM samples and normal skin tissues. Genes with a FDR < 0.05 and |log2 fold change (FC)| > 1 were regarded as candidate DEOGs based on previous methods[42] and were visualized using a volcano plot using the "ggplot2" package[43]. Furthermore, genes that were overlapping between candidate DEOGs, the WGCN and GSE65904 were con-

sidered as "real" DEOGs and were visualized using a Venn diagram generated by the "VennDiagram" package[44].

### Construction of A Prognostic Model and Evaluation of Its Efficacy

All DEOGs were subjected to univariate Cox regression analysis using the "survival" package with a cutoff criterion of $p < 0.05$. Thereafter, genes from this analysis were integrated into LASSO analysis[45] to select hub OS genes and generate a SKCM risk model. Next, SKCM patients were categorized into high - and low-risk subgroups. Risk score of each sample was calculated as follows:

$$\text{Risk score} = \Sigma \text{expgenei} * \beta i$$

where expgenei represents the relative expression value of OS gene i and β represents the regression coefficient[46]. The "survival" package was integrated into the Kaplan-Meier method and log-rank test to compare outcomes between the two risk subgroups. The "survivalROC" and "timeROC" packages were used to validate predictive accuracy of the gene signature[47]. Univariate and multivariate Cox regression analyses evaluated the relationship between clinical characteristics and risk score, with a nomogram incorporating calibration plots and using the "rms" package was generated to determine clinical outcomes of SKCM patients[48].

### Evaluation of Hub Genes

The HPA online database (http://www.proteinatlas.org/) was used to determine protein expression differences between normal skin and SKCM tumor tissues[49,50]. These data were analyzed using Image-J software (National Institutes of Health, Bethesda, MD, USA), which quantified the percentage of positive staining. Gene expression levels of key OS genes were confirmed using TCGA dataset. The prognostic value of each gene situated in the TCGA-SKCM cohort was determined using the Kaplan-Meier method.

### GO and KEGG Enrichment Analyses

The Database for Annotation, Visualization and Integrated Discovery version 6.8[51] was used to determine the biological functions of hub OS genes. Three terms including BP, CC, and MF were used in GO analyses. Both $p$ and FDR values of $< 0.05$ were considered to be statistically significant.

### Statistical Analysis

All statistical analyses were performed with SPSS (Statistical Product and Service Solution) software version 23.0 ((IBM Corp., Armonk, NY, USA)[52]. Measurement data were presented as the mean ± SD (standard deviation), and the difference between risk score and clinical features were compared with Student's $t$-test and $\chi^2$-test. Furthermore, log rank test was also applied for Kaplan-Meier survival analysis, and multivariate Cox regression analysis was used to determine whether our constructed risk model was independent of other clinical characters. $p$-values of $< 0.05$ were considered statistically significant.

## Results

### New Hub Modules Using WGCN

Publicly available datasets were analyzed as presented in Figure 1. To identify functional clusters in SKCM patients, WGCNA was performed on 471 SKCM samples that contained clinical information provided by the TCGA-SKCM cohort related to 1399 extracted OS genes. The $\beta = 12$ (scale-free $R^2 = 0.85$) was used as a soft-threshold for the scale-free network (Figure 2A). Four co-expressed modules were identified (Figure 2B-C) and each was assigned a different color to identify connections with normal or

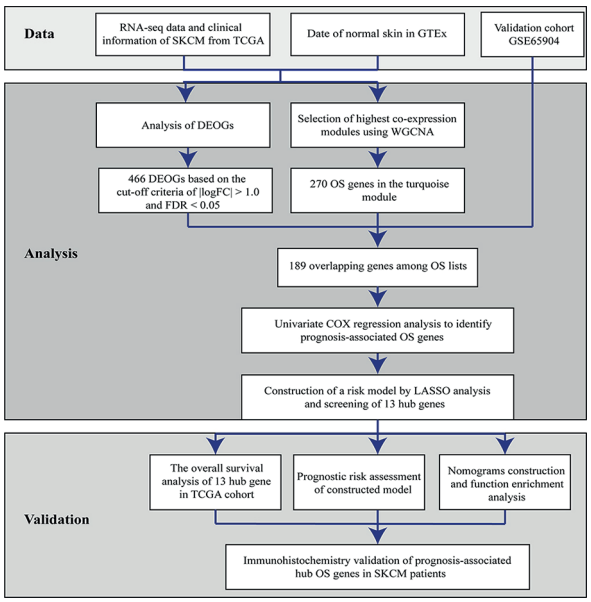


**Figure 1.** Flowchart describing the schematic overview of the study design.

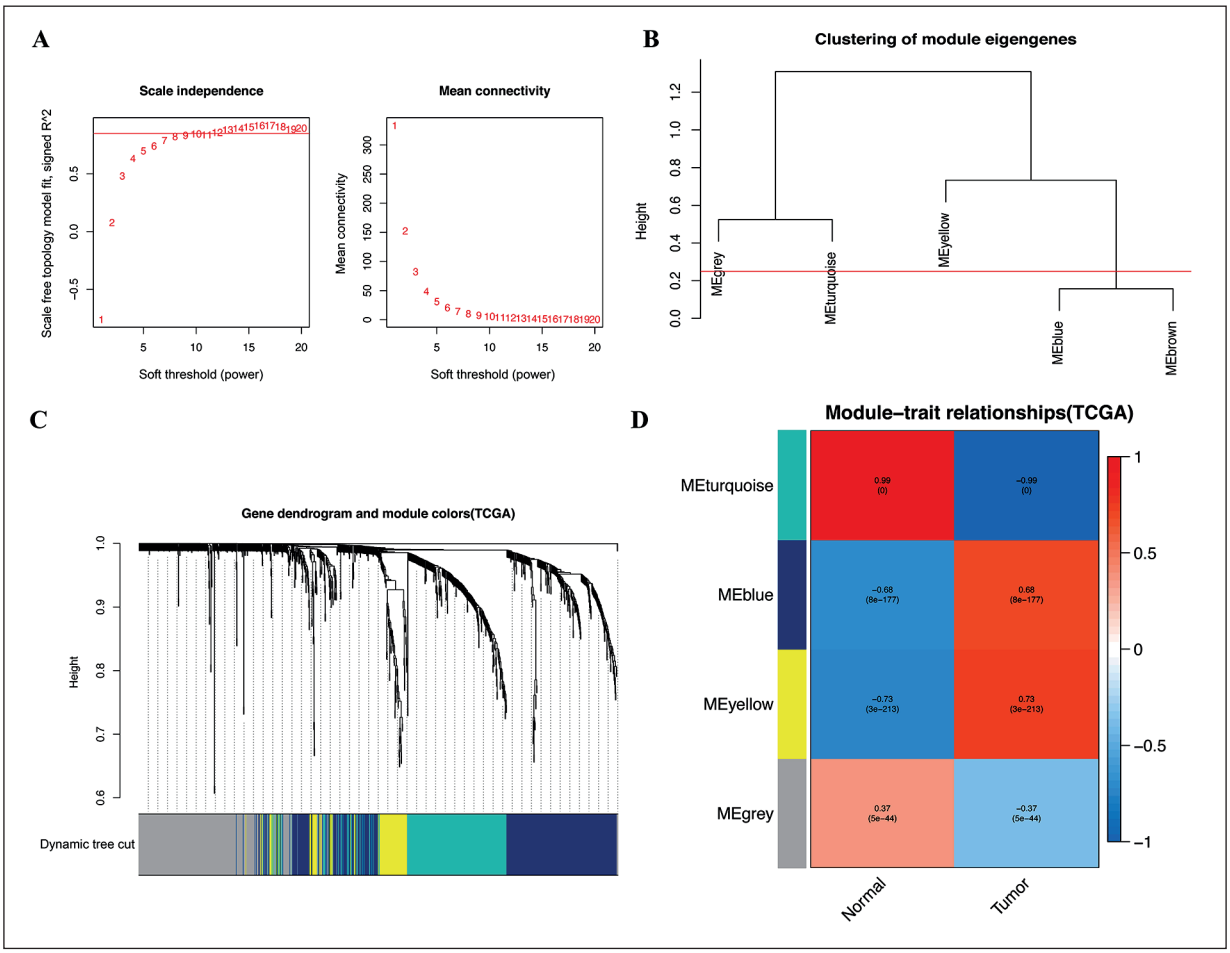


**Figure 2.** Identification of modules associated with the clinical information in the TCGA-SKCM dataset. **A,** The scale-free fit index for soft-thresholding powers. **B,** Clustering of modules eigengenes. **C,** A dendrogram of co-expression network modules was ordered by a hierarchical clustering of genes. Each module was assigned with different colors. **D,** A heatmap showing the correlation between the gene module and clinical trait (tumor and normal). The correlation coefficient in each cell represented the correlation between gene module and the clinical traits, which decreased in size from red to blue.

tumor traits. The turquoise module was positively associated with normal tissues (r = 0.99, $p = 0$; Figure 2D) and selected as the module of interest.

## Overlapping DEOGs

Based on a false discovery rate (FDR) < 0.05 and |logFC| > 1.0, a total of 466 OS genes were identified in the TCGA dataset. There were 228 genes that were downregulated and 238 genes that were upregulated and identified as candidate DEOGs (Figure 3A). Figure 3B reveals the distribution of co-expression genes from DEOGs, the turquoise module from TCGA and GSE65904 gene sets. A total of 189 overlapping genes were used for further analyses.

## Prognosis-Associated OS Gene Screening and Genetic Risk Score Model Construction for SKCM Patients

The 189 identified DEOGs were further analyzed using univariate Cox regression analysis. A total of 17 OS genes were identified with a $p < 0.05$ (Figure 4A). The LASSO algorithm was used to shrink the OS gene range (Figure 4B and C) and 13 hub OS genes (*MMP2, STK25, TUFM, C4B, EGFR, CARS2, ACOX2, GLE1, MGST1, CALM2, UBQLN4, A2M,* and *FAS*) were selected to determine the risk score. Using median risk scores, all SKCM patients in the TCGA (Figure 4D) and GSE65904 (Figure 4E) cohorts were divided into low- and high-risk groups. Coefficients of 13 hub genes are provided in Table I.

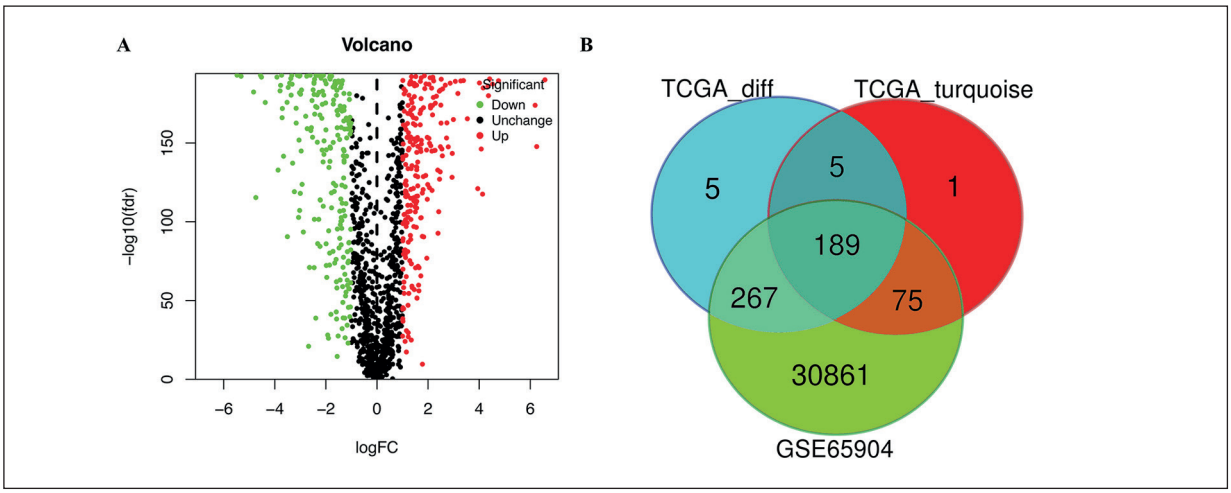


**Figure 3.** Identification of DEOGs among the TCGA and GSE65904 cohorts of SKCM. **A,** Volcano plot of candidate DEOGs in the TCGA dataset with the cut-off criteria of FDR < 0.05 and |logFC| > 1. **B,** The Venn diagram of genes among candidate DEOG, WGCN, and GSE65904 lists.

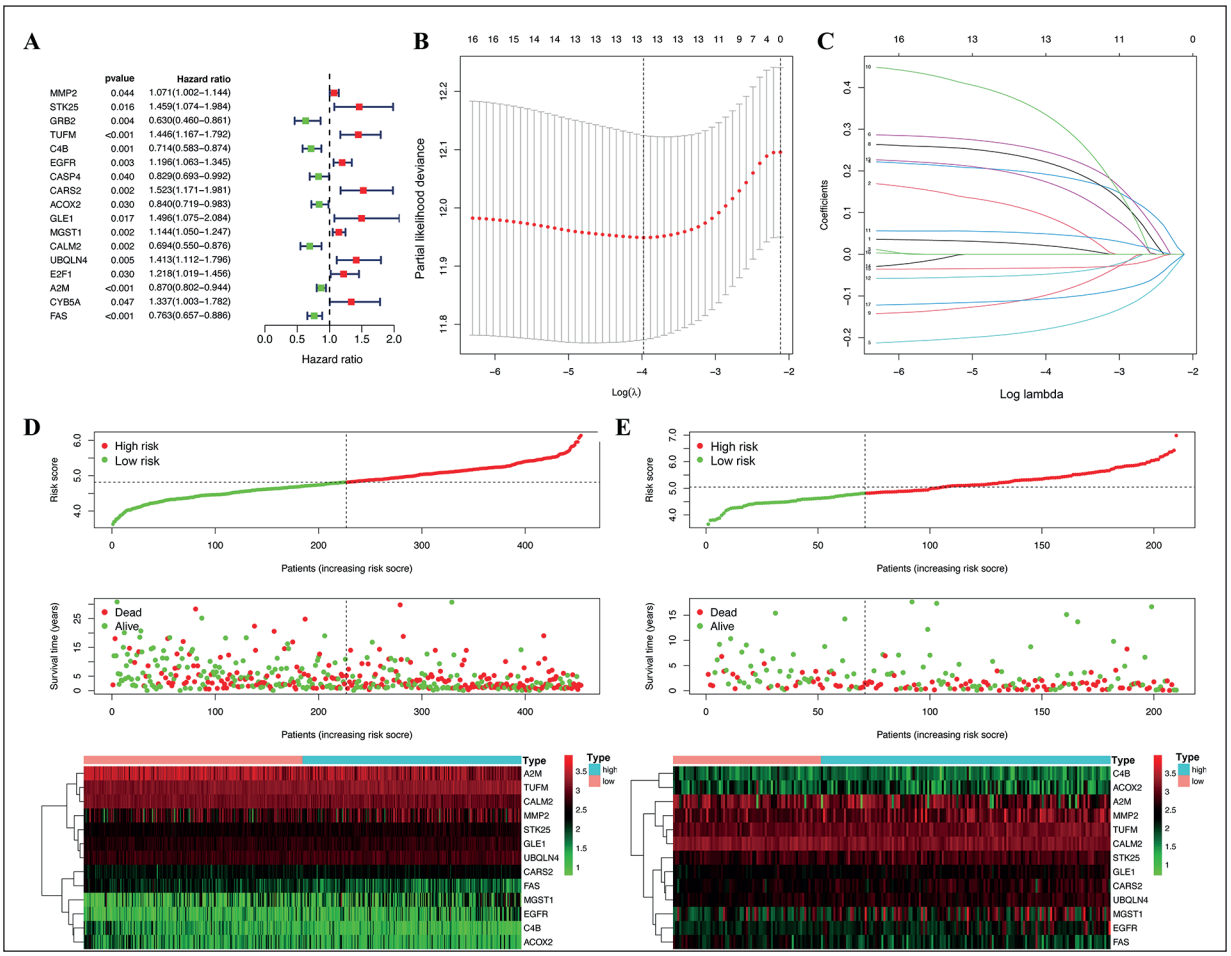


**Figure 4.** Construction of prognostic model in the TCGA and GSE65904 cohorts. **A,** Univariate Cox regression analysis for identifying prognosis-related OS genes in TCGA cohort. **B-C,** LASSO analysis for determining the number of factors and constructing the prognosis prediction model. **D,** Risk score distribution, survival status, and expression heat map of TCGA cohort. **E,** Risk score distribution, survival status, and expression heat map of GSE65904 cohort.

**Table I.** 13 prognosis-associated OS genes with SKCM in the TCGA dataset were identified by LASSO analysis.

| OS name | HR | Univariate Cox regression analysis | | | LASSO coefficient |
|---|---|---|---|---|---|
| | | Lower 95% CI | Upper 95% CI | *p*-value | |
| MMP2 | 1.07051242 | 1.00185395 | 1.14387615 | 0.04393273 | 0.0206 |
| STK25 | 1.45938553 | 1.07362146 | 1.9837589 | 0.01579938 | 0.0905 |
| TUFM | 1.44611954 | 1.16715556 | 1.79175921 | 0.00074206 | 0.1915 |
| C4B | 0.7135384 | 0.58282892 | 0.87356174 | 0.00107801 | -0.1790 |
| EGFR | 1.19578109 | 1.06303628 | 1.34510217 | 0.00289988 | 0.2453 |
| CARS2 | 1.52264663 | 1.17062463 | 1.9805262 | 0.0017222 | 0.2199 |
| ACOX2 | 0.84044443 | 0.71861297 | 0.98293081 | 0.02959785 | -0.0972 |
| GLE1 | 1.49630354 | 1.07454398 | 2.08360412 | 0.0170533 | 0.3325 |
| MGST1 | 1.14437718 | 1.05029274 | 1.24688964 | 0.00206324 | 0.0487 |
| CALM2 | 0.69373683 | 0.54970193 | 0.87551227 | 0.00207243 | -0.0474 |
| UBQLN4 | 1.41294664 | 1.11171252 | 1.79580438 | 0.00471891 | 0.1726 |
| A2M | 0.86973665 | 0.80156876 | 0.94370176 | 0.00080398 | -0.0329 |
| FAS | 0.7627499 | 0.65669253 | 0.88593578 | 0.00039191 | -0.1067 |

### Prognostic Risk Score and Clinical Characteristics Associations in SKCM Patients

Overall survival of SKCM patients significantly decreased with a higher risk score in the TCGA cohort (Figure 5A). Both univariate and multivariate Cox regression analyses revealed an association between risk score and SKCM prognosis. These analyses also revealed that risk score can be an independent prognostic feature for SKCM patients (Figure 5C and D). Additionally, receiver operating characteristic (ROC) analysis of overall survival in SKCM patients indicated that our model contained a moderate predictive accuracy ROC curve >0.728 at 7 years in the TCGA database (Figure 5B), suggesting that this model is more accurate than other others (Figure 5I). Findings were also confirmed using the GSE65904 cohort (Figure 5E-H and J), demonstrating our model was both specific and sensitive for the analysis of SKCM patients.

Furthermore, patients in the age group of >60 years of age or patients diagnosed with primary melanoma showed significant associations with higher risk scores ($p < 0.05$, Figure 6A and C). It was also uncovered that cancers with higher T stages showed significantly greater risk scores ($p < 0.05$, Figure 6B). This suggested that this risk model is linked to the progression of SKCM patients. Heatmaps of the TCGA and GSE65904 cohorts were generated to reveal expression levels of 13 hub OS genes (Figure 6D-E). These data revealed significant differences in the two groups in respect to metastasis, as well as TNM and T stages in the TCGA cohort and tumor stage in the GSE65904 cohort ($p < 0.05$).

### Prognostic Value of Selected Hub OS Genes

Significantly elevated expression levels were identified for *TUFM, GLE1, UBQLN4* and *A2M* in SKCM samples. In contrast, a significant decrease in the expression levels of *MMP2, STK25, C4B, EGFR, CARS2, ACOX2, MGST1, CALM2* and *FAS* were observed in SKCM versus normal skin samples (**Supplementary Figure 1**). Immunohistochemistry data provided by the Human Protein Atlas (HPA) database were used to confirm protein expression levels of OS genes (Figure 7A-M). Next, the prognostic value of the selected OS genes was interrogated using Kaplan-Meier survival analysis. This revealed that overall survival of SKCM patients was negatively associated with *MMP2, STK25, TUFM, UBQLN4, EGFR, CARS2, GLE1,* and *MGST1* expression levels (Figure 7A-H, $p < 0.05$). Prognosis was positively associated with *CALM2, A2M, FAS, ACOX2,* and *C4B* expression levels ($p < 0.05$, Figure 7I-M).

### Functional Enrichment Analysis

Hub genes were found to be enriched in response to OS, ROS, protein autophosphorylation and the stress-activated MAPK cascade using Gene Ontology (GO) enrichment analysis (Figure 8A). Kyoto Encyclopedia of Genes and Genomes (KEGG) enrichment analysis portrayed that selected hub genes were enriched in the GnRH, estrogen, fluid shear stress and atherosclerosis pathways (Figure 8B). Furthermore, KEGG enrichment analysis also indicated that the hub genes not only were significantly as-

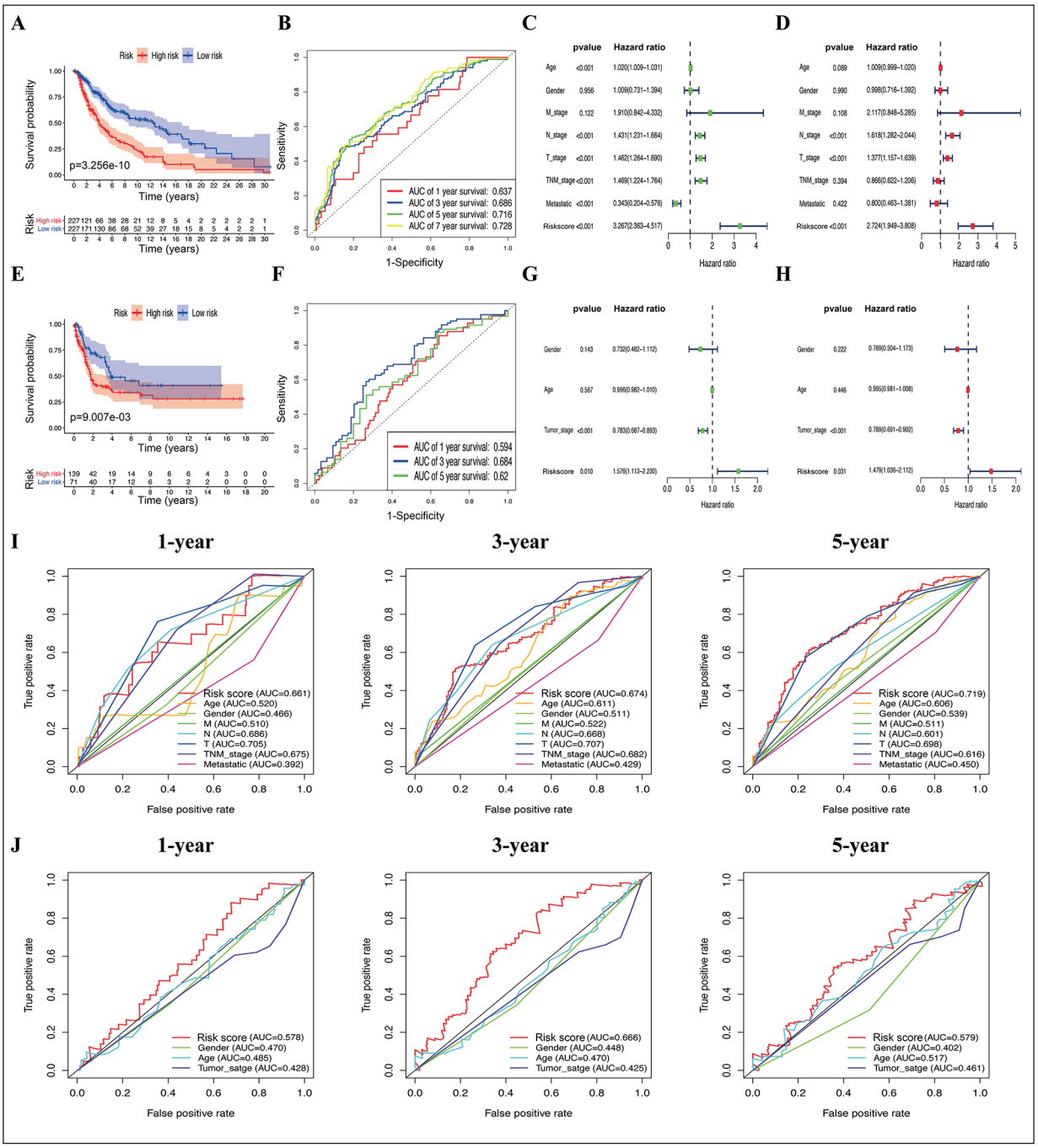


**Figure 5.** Efficacy evaluation of constructed prognostic model. **A,** Survival curve of TCGA cohort. **B,** TimeROC curves for forecasting overall survival in TCGA cohort. Univariate and multivariate Cox regression analysis of the clinicopathological features in TCGA (**C-D**) and GSE65904 (**G-H**) cohorts. (**E**) Survival curve of GSE65904 cohort. (**F**) TimeROC curves for forecasting overall survival in GSE65904 cohort. ClinicalROC curves for forecasting overall survival in TCGA (**I**) and GSE65904 (**J**) cohort.

sociated with SKCM prognosis but also played a critical role in other cancer types including bladder cancer and glioma. This led us into further exploring the role of these OS genes in other tumor types.

### *Nomogram Construction*

Both risk score and clinical characteristics were used to construct nomogram plots predicting outcomes and overall survival of SKCM patients in both the TCGA and GSE65904

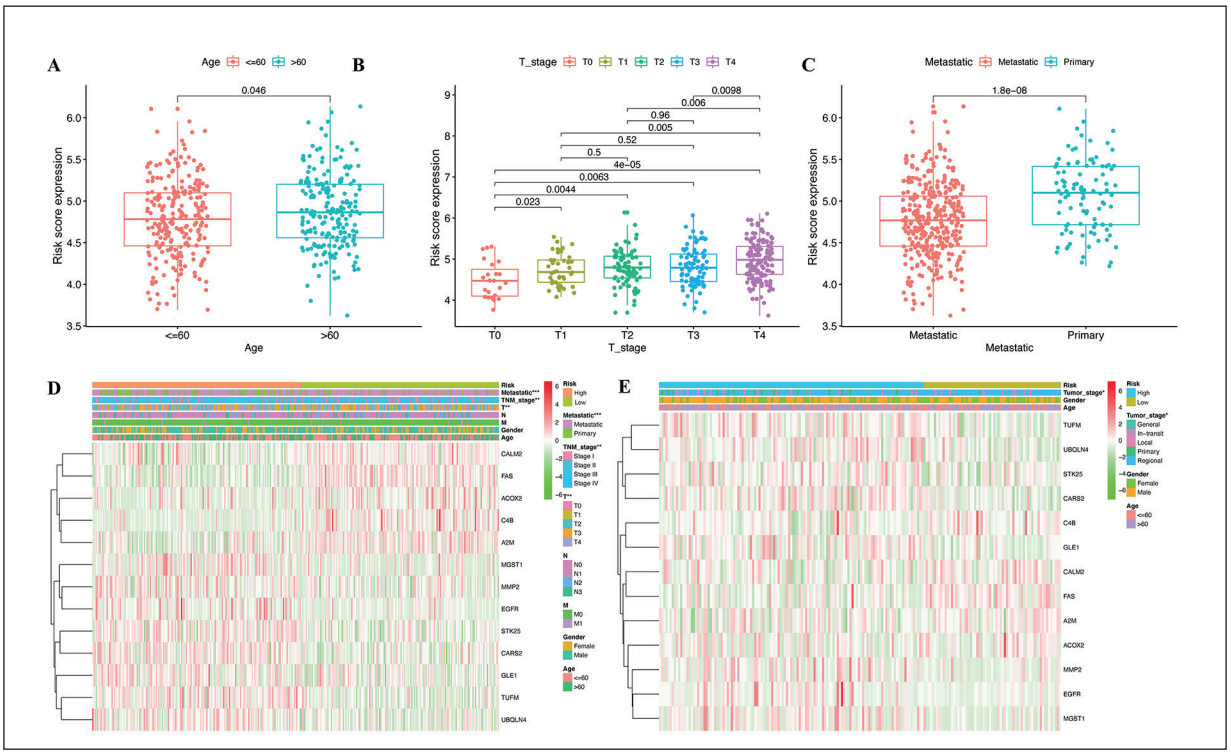


**Figure 6.** Evaluation the relationship between the risk score and clinicopathological parameters in patients with SKCM. Correlation analysis between the risk score and clinicopathological characters of Age (**A**), T stage (**B**), and metastatic ability (**C**) in TCGA cohort. The heatmap shows the distribution of clinicopathological features and OS genes expression in two risk subgroups from the TCGA (**D**) and GSE65904 (**E**) cohorts.

cohorts (Figure 9A and C). Our prognostic risk model showed that calibration plots at 3 and 5 years demonstrated strong conformity (Figure 9B and D). Expression levels of 13 hub genes in the TCGA and GSE65904 cohorts were also used to generate nomogram plots (Figure 10A and C). Predicted and observed outcomes showed strong conformity based on respective calibration plots (Figure 10B and D).

## Discussion

Despite the discovery of new biomarkers for melanoma, there is still a need for novel markers more closely associated with early diagnosis and prognosis of SKCM[53]. In the study presented here, a co-expression network of OS genes was generated, and differential expression analysis was applied to identify the differentially expressed OS genes (DEOGs). Next, univariate Cox regression and LASSO analyses were used to identify 13 differentially expressed OS genes including *MMP2, STK25, TUFM, C4B, EGFR, CARS2, ACOX2, GLE1, MGST1, CALM2, UBQLN4, A2M,* and *FAS*, as hub prognosis-associated genes. *TUFM, GLE1, UBQLN4* and *A2M* were overexpressed and *MMP2, STK25, C4B, EGFR, CARS2, ACOX2, MGST1, CALM2* and *FAS* were decreased in SKCM tissues. In addition, *MMP2, STK25, TUFM, UBQLN4, EGFR, CARS2, GLE1,* and *MGST1* were found to be negatively associated with overall survival of SKCM patients. In contrast, *CALM2, A2M, FAS, ACOX2*, and *C4B* were positively correlated with patient outcomes. Ubiquitously and abundantly expressed in most cells, *MMP2*, which encodes a gelatinase that primarily degenerates collagen type IV, is reportedly activated by OS[54], ultimately promoting melanoma progression[55]. Furthermore, *MMP2* overexpression is significantly associated with atypia progression and architectural impairment[56,57]. In skin cancer, the *EGFR* ligand is transactivated by the overproduction of ROS[58,59]. Overexpression of *MGST1* (a member of the antioxidant system) protects cells from ROS damage and leads to less metastasis in melanoma[60]. The *FAS*-ligand is preferentially expressed

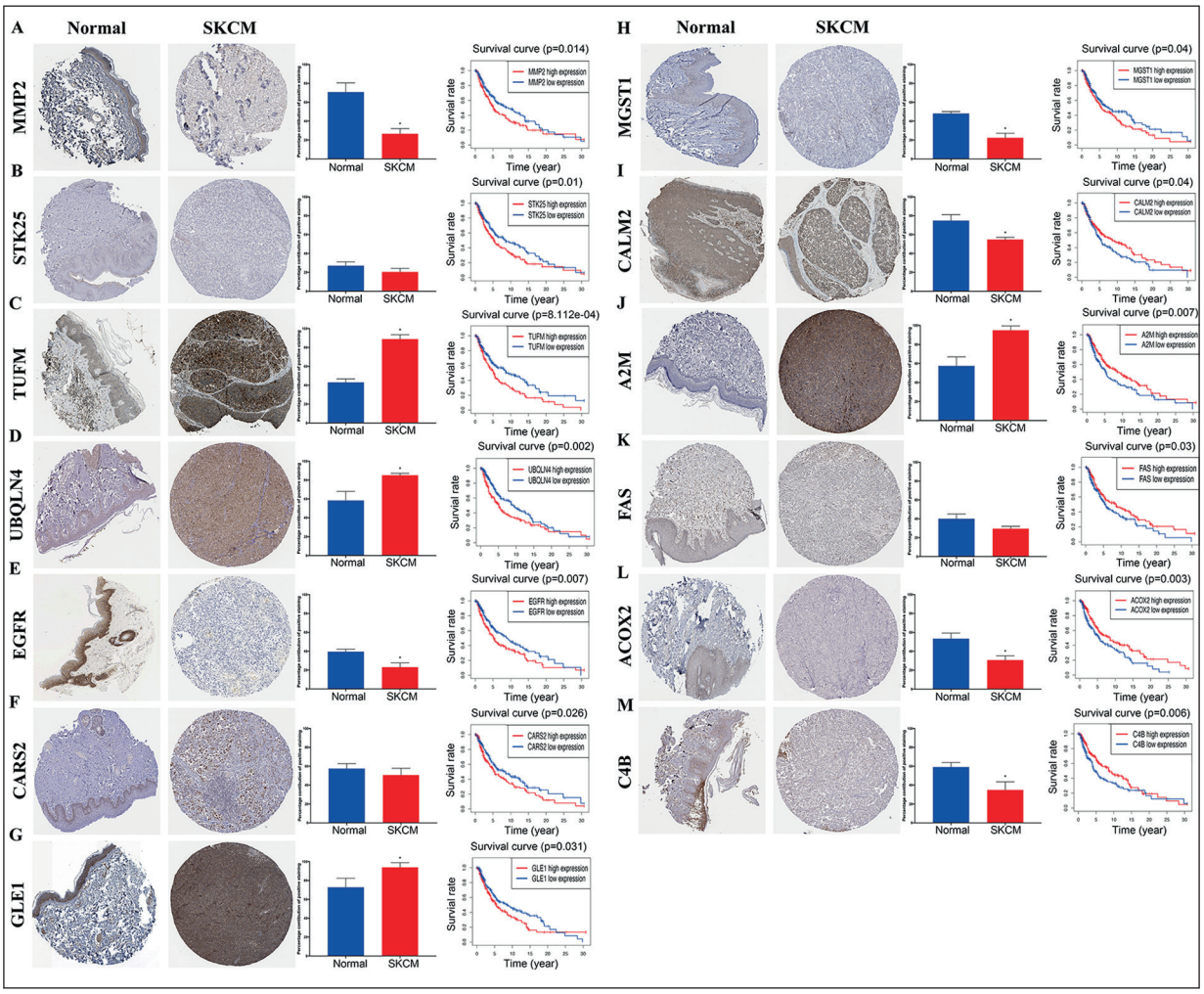


**Figure 7.** HPA database and Kaplan-Meier analysis in TCGA cohort verified the protein expression and prognostic value of MMP2 (**A**), STK25 (**B**), TUFM (**C**), UBQLN4 (**D**), EGFR (**E**), CARS2 (**F**), GLE1 (**G**), MGST1 (**H**), CALM2 (**I**), A2M (**J**), FAS (**K**), ACOX2 (**L**), and C4B (**M**) in SKCM. Values are presented as means ± standard deviation (n=3), *$p < 0.05$ relative to the control group. Magnification ×200.

in the basal layer of the epidermis and functions as a surveillance molecule involved in preventing cell transformation[61] and promoting cellular ROS generation through NADPH oxidase activation[62]. *FAS* is also involved in apoptotic processes[63] and its decreased expression was significantly linked to a poor prognosis in cases of malignant melanoma[64]. Some of the identified hub genes in our study were previously significantly associated with SKCM progression. However, there are no studies systematically analyzing the specific prognostic role of OS genes in SKCM. Therefore, our analysis provides insight into the relationship between OS and SKCM progression, identifying valuable OS-associated biomarkers for personalized treatment.

In this study, a new prognostic prediction model was constructed to determine whether they could be used as prognostic markers, generating the first OS-associated risk model for SKCM prognosis. Both univariate and multivariate Cox regression analyses indicate the reliable prognostic value for SKCM if this model is used. Our model also is successful in predicting SKCM prognosis and has shown to have increased accuracy compared to features such as age, gender, TNM stage and metastatic ability. In addition, we considered the role of OS in the stages of cancer progression and carcinogenesis[65,66] by assessing connections between risk score and SKCM clinical factors. Our model was significantly associated with metastasis, T

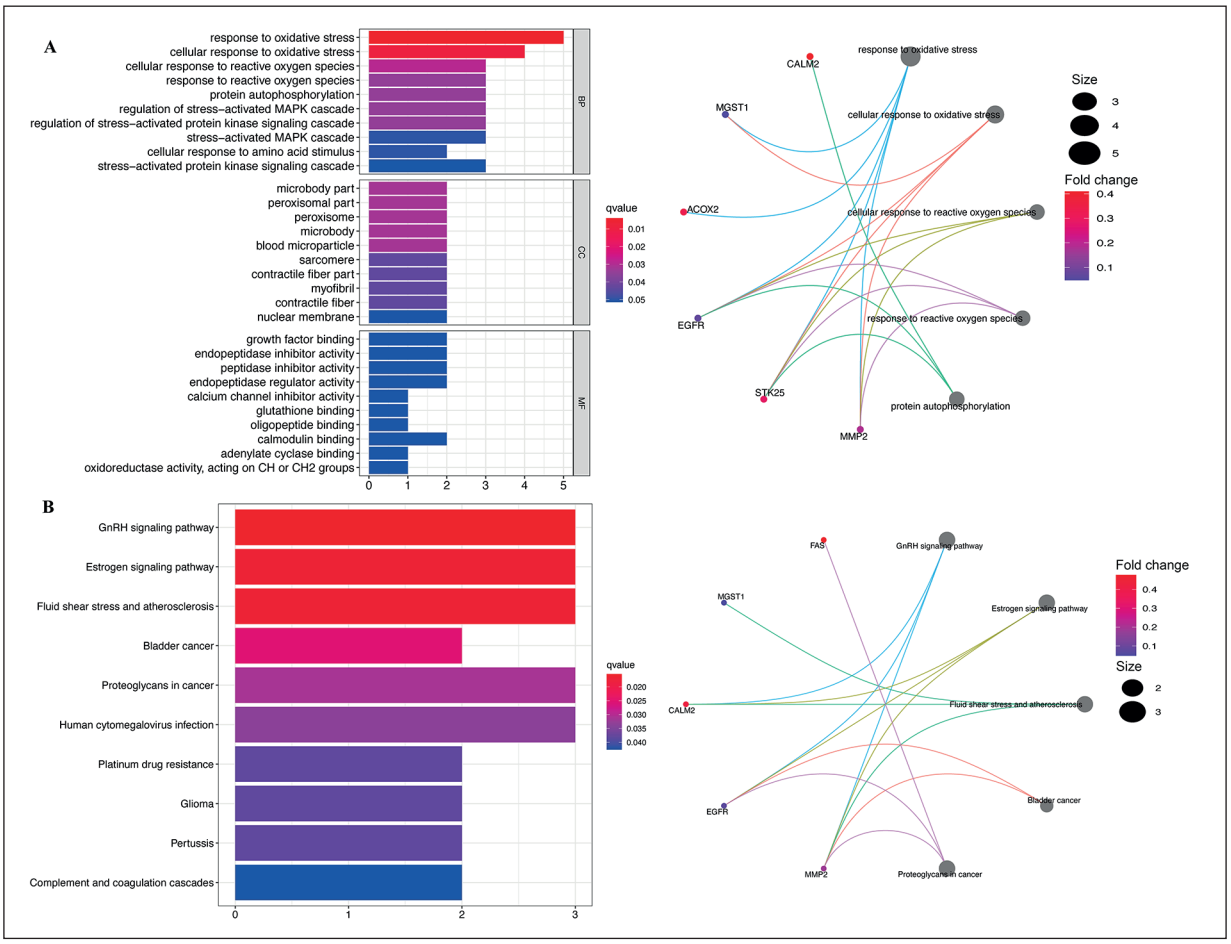


**Figure 8.** Functional enrichment analysis. **A,** GO enrichment terms of hub OS genes in biological process (BP), cellular component (CC), and molecular function (MF). **B,** KEGG enrichment terms of hub OS genes. In each bubble plot, the size of the dot represents the number of enriched genes.

stage and patient age. As one of the most widely used clinicopathological parameters, the American Joint Committee on Cancer (AJCC) staging system was also used for the prediction of SKCM prognosis[4]. However, there is increasing evidence supporting the notion that the AJCC staging model is still not suitable for the comprehensive elucidation of tumor behavior and is not accurate in diagnostics[67]. A similar conclusion was made in this study for SKCM patients. Compared with TNM stage in SKCM, our risk model not only showed a stronger relationship with SKCM prognosis, but also predicted SKCM progression, including tumor growth and metastatic potential. Nomogram analysis revealed how credible this risk signature was in predicting SKCM patient overall survival.

Nonetheless, despite these findings, there were still certain limitations in this study. First, a retrospective analysis was performed, and in the future, a prospective approach should be used to confirm the results presented here. Second, there was a lack of experiments performed to confirm the mechanisms we uncovered through bioinformatics. Therefore, in the future, experiments need to be performed to achieve mechanistic insight for the identified genes and their relation to the progression of SKCM.

## Conclusions

In summary, we constructed a co-expression network and performed bioinformatic analyses to identify 13 hub OS genes significantly associated with the overall survival of patients with SKCM. We also successfully constructed a prognostic model with powerful predictive effects. To the

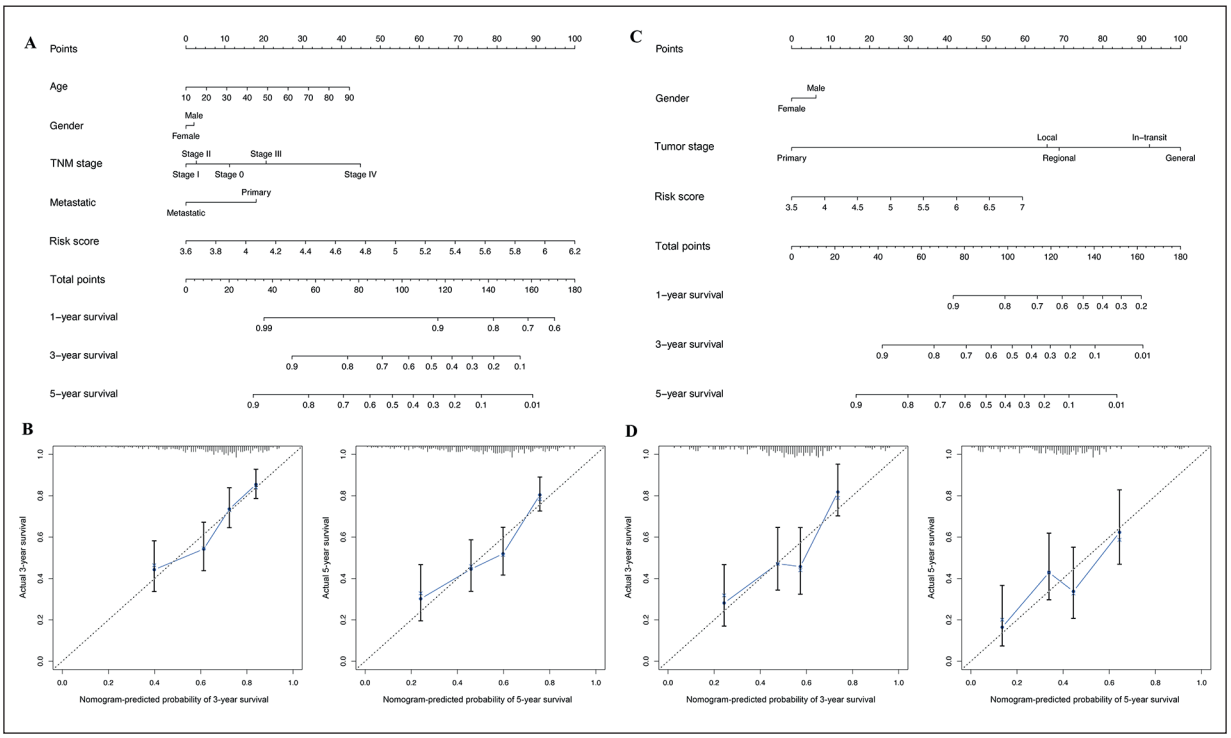


**Figure 9.** Construction of nomogram based on the risk score and other clinical factors. Nomograms for predicting SKCM 1-, 3-, and 5-year overall survival in TCGA (**A**) and GSE65904 (**C**) cohort. **B,** The calibration plot of the nomogram in TCGA cohort. **D,** The calibration plot of the nomogram in GSE65904 cohort.

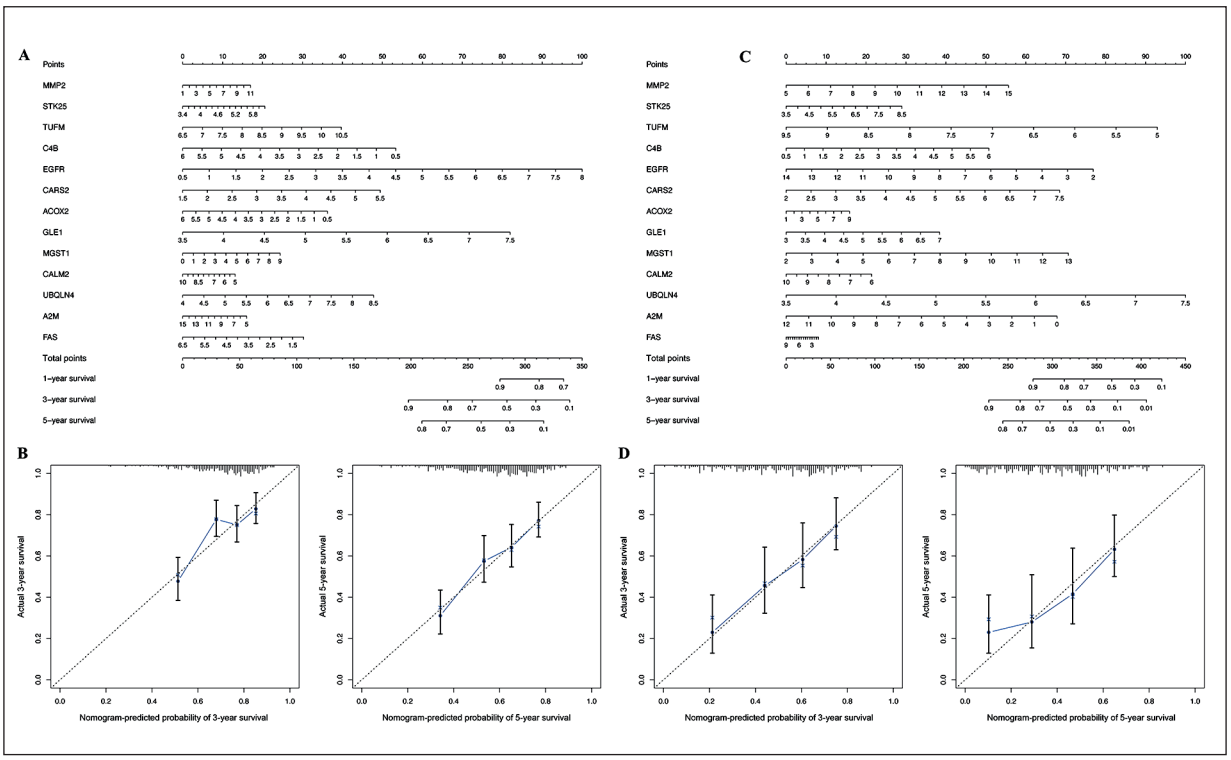


**Figure 10.** Construction of nomogram based on the expression of 13 OS genes. The nomogram (**A**) and calibration plot (**B**) of 13 OS genes in TCGA cohort. The nomogram (**C**) and calibration plot (**D**) of 13 OS genes in GSE65904 cohort.

best of our knowledge, this is the first OS-associated model to predict the prognosis of SKCM malignancy. This work identified a new method for understanding the specific roles of OS in SKCM and highlighted the potential of OS profiling to elucidate clinical prognosis in SKCM patients. We believe that our study makes a significant contribution to the literature as our prognostic model may provide new insights into the pathogenesis, prognosis, and individualized treatment in patients with SKCM.

### Conflict of Interest

The Authors declare that they have no conflict of interests.

### Acknowledgements

We acknowledge and appreciate our colleagues for their valuable efforts and comments on this paper.

### Authors' Contribution

Conceived and designed the experiments: TR. Performed the experiments: YZ. Analyzed the data: TR. Contributed reagents/materials/analysis tools: YZ. Wrote the paper: WH.

### Data Availability Statement

The datasets analysed during the current study are available sourced from the publicly available TCGA, GTEx, GEO, and HPA database (https://portal.gdc.cancer.gov, https://gtexportal.org/home/datasets, https://www.ncbi.nlm.nih.gov/geo/, http://www.proteinatlas.org/).

## References

1) Ekwueme DU, Guy GP, Jr., Li C, Rim SH, Parelkar P, Chen SC. The health burden and economic costs of cutaneous melanoma mortality by race/ethnicity-United States, 2000 to 2006. J Am Acad Dermatol 2011; 65: S133-143.
2) Bray F, Ferlay J, Soerjomataram I, Siegel RL, Torre LA, Jemal A. Global cancer statistics 2018: GLOBOCAN estimates of incidence and mortality worldwide for 36 cancers in 185 countries. CA Cancer J Clin 2018; 68: 394-424.
3) Finn L, Markovic SN, Joseph RW. Therapy for metastatic melanoma: the past, present, and future. BMC Med 2012; 10: 23.
4) Gershenwald JE, Scolyer RA, Hess KR, Sondak VK, Long GV, Ross MI, Lazar AJ, Faries MB, Kirkwood JM, McArthur GA, Haydu LE, Eggermont AMM, Flaherty KT, Balch CM, Thompson JF. Melanoma staging: Evidence-based changes in the American Joint Committee on Cancer eighth edition cancer staging manual. CA Cancer J Clin 2017; 67: 472-492.
5) Hamm C, Verma S, Petrella T, Bak K, Charette M. Biochemotherapy for the treatment of metastatic malignant melanoma: a systematic review. Cancer Treat Rev 2008; 34: 145-156.
6) Board PDQATE. Melanoma Treatment (PDQ®): Health Professional Version. In: PDQ Cancer Information Summaries. Bethesda (MD): National Cancer Institute (US); 2002.
7) Kanavy HE, Gerstenblith MR. Ultraviolet radiation and melanoma. Semin Cutan Med Surg 2011; 30: 222-228.
8) Gilchrest BA, Eller MS, Geller AC, Yaar M. The pathogenesis of melanoma induced by ultraviolet radiation. N Engl J Med 1999; 340: 1341-1348.
9) Hawkes JE, Truong A, Meyer LJ. Genetic predisposition to melanoma. Semin Oncol 2016; 43: 591-597.
10) Jang S, Atkins MB. Treatment of BRAF-mutant melanoma: the role of vemurafenib and other therapies. Clin Pharmacol Ther 2014; 95: 24-31.
11) Yang S, Leone DA, Biswas A, Deng A, Jukic D, Singh R, Sundram U, Mahalingam M. Concordance of somatic mutation profiles (BRAF, NRAS, and TERT) and tumoral PD-L1 in matched primary cutaneous and metastatic melanoma samples. Hum Pathol 2018; 82: 206-214.
12) Wang HZ, Wang F, Chen PF, Zhang M, Yu MX, Wang HL, Zhao Q, Liu J. Coexpression network analysis identified that plakophilin 1 is associated with the metastasis in human melanoma. Biomed Pharmacother 2019; 111: 1234-1242.
13) Lü JM, Lin PH, Yao Q, Chen C. Chemical and molecular mechanisms of antioxidants: experimental approaches and model systems. J Cell Mol Med 2010; 14: 840-860.
14) Zhou F, Pan Y, Wei Y, Zhang R, Bai G, Shen Q, Meng S, Le XF, Andreeff M, Claret FX. Jab1/Csn5-Thioredoxin Signaling in Relapsed Acute Monocytic Leukemia under Oxidative Stress. Clin Cancer Res 2017; 23: 4450-4461.
15) Brown JM, Wilson WR. Exploiting tumour hypoxia in cancer treatment. Nat Rev Cancer 2004; 4: 437-447.
16) Kangari P, Zarnoosheh Farahany T, Golchin A, Ebadollahzadeh S, Salmaninejad A, Mahboob SA, Nourazarian A. Enzymatic Antioxidant and Lipid Peroxidation Evaluation in the Newly Diagnosed Breast Cancer Patients in Iran. Asian Pac J Cancer Prev 2018; 19: 3511-3515.
17) Liu-Smith F, Dellinger R, Meyskens FL, Jr. Updates of reactive oxygen species in melanoma etiology and progression. Arch Biochem Biophys 2014; 563: 51-55.
18) Wang JY, Liu GZ, Wilmott JS, La T, Feng YC, Yari H, Yan XG, Thorne RF, Scolyer RA, Zhang XD, Jin L. Skp2-mediated stabilization of MTH1 promotes survival of melanoma cells upon oxidative stress. Cancer Res 2017; 77: 6226-6239.

19) Zhou F, Shen Q, Claret FX. Novel roles of reactive oxygen species in the pathogenesis of acute myeloid leukemia. J Leukoc Biol 2013; 94: 423-429.
20) Oates JC, Gilkeson GS. The biology of nitric oxide and other reactive intermediates in systemic lupus erythematosus. Clin Immunol 2006; 121: 243-250.
21) Smith J, Tho LM, Xu N, Gillespie DA. The ATM-Chk2 and ATR-Chk1 pathways in DNA damage signaling and cancer. Adv Cancer Res 2010; 108: 73-112.
22) Denat L, Kadekaro AL, Marrot L, Leachman SA, Abdel-Malek ZA. Melanocytes as instigators and victims of oxidative stress. J Invest Dermatol 2014; 134: 1512-1518.
23) Obrador E, Liu-Smith F, Dellinger RW, Salvador R, Meyskens FL, Estrela JM. Oxidative stress and antioxidants in the pathophysiology of malignant melanoma. Biol Chem 2019; 400: 589-612.
24) Jenkins NC, Grossman D. Role of melanin in melanocyte dysregulation of reactive oxygen species. Biomed Res Int 2013; 2013: 908797.
25) Qiu T, Wang H, Wang Y, Zhang Y, Hui Q, Tao K. Identification of genes associated with melanoma metastasis. Kaohsiung J Med Sci 2015; 31: 553-561.
26) Haqq C, Nosrati M, Sudilovsky D, Crothers J, Khodabakhsh D, Pulliam BL, Federman S, Miller JR, 3rd, Allen RE, Singer MI, Leong SP, Ljung BM, Sagebiel RW, Kashani-Sabet M. The gene expression signatures of melanoma progression. Proc Natl Acad Sci U S A 2005; 102: 6092-6097.
27) Udyavar AR, Hoeksema MD, Clark JE, Zou Y, Tang Z, Li Z, Li M, Chen H, Statnikov A, Shyr Y, Liebler DC, Field J, Eisenberg R, Estrada L, Massion PP, Quaranta V. Co-expression network analysis identifies Spleen Tyrosine Kinase (SYK) as a candidate oncogenic driver in a subset of small-cell lung cancer. BMC Syst Biol 2013; 7 Suppl 5: S1.
28) Yang L, Xu Y, Yan Y, Luo P, Chen S, Zheng B, Yan W, Chen Y, Wang C. Common Nevus and Skin Cutaneous Melanoma: Prognostic Genes Identified by Gene Co-Expression Network Analysis. Genes (Basel) 2019; 10: 747.
29) Wan Q, Tang J, Han Y, Wang D. Co-expression modules construction by WGCNA and identify potential prognostic markers of uveal melanoma. Exp Eye Res 2018; 166: 13-20.
30) Segundo-Val IS, Sanz-Lozano CS. Introduction to the Gene Expression Analysis. Methods Mol Biol 2016; 1434: 29-43.
31) Li B, Severson E, Pignon JC, Zhao H, Li T, Novak J, Jiang P, Shen H, Aster JC, Rodig S, Signoretti S, Liu JS, Liu XS. Comprehensive analyses of tumor immunity: implications for cancer immunotherapy. Genome Biol 2016; 17: 174.
32) Xin X, Zhang Y, Ling F, Wang L, Sheng X, Qin L, Zhao X. Identification of a nine-miRNA signature for the prognosis of Uveal Melanoma. Exp Eye Res 2019; 180: 242-249.
33) Tian J, Yang Y, Li MY, Zhang Y. A novel RNA sequencing-based prognostic nomogram to predict survival for patients with cutaneous melanoma: Clinical trial/experimental study. Medicine (Baltimore) 2020; 99: e18868.
34) Sun L, Li P, Ren H, Liu G, Sun L. A four-gene expression-based signature predicts the clinical outcome of melanoma. J Buon 2019; 24: 2161-2167.
35) Liu J, Li R, Liao X, Hu B, Yu J. Comprehensive investigation of the clinical significance and molecular mechanisms of plasmacytoma variant translocation 1 in sarcoma using genome-wide RNA sequencing data. J Cancer 2019; 10: 4961-4977.
36) Human genomics. The Genotype-Tissue Expression (GTEx) pilot analysis: multitissue gene regulation in humans. Science 2015; 348: 648-660.
37) Gentles AJ, Newman AM, Liu CL, Bratman SV, Feng W, Kim D, Nair VS, Xu Y, Khuong A, Hoang CD, Diehn M, West RB, Plevritis SK, Alizadeh AA. The prognostic landscape of genes and infiltrating immune cells across human cancers. Nat Med 2015; 21: 938-945.
38) Huang R, Mao M, Lu Y, Yu Q, Liao L. A novel immune-related genes prognosis biomarker for melanoma: associated with tumor microenvironment. Aging (Albany NY) 2020; 12: 6966-6980.
39) Zhang M, Wang X, Chen X, Zhang Q, Hong J. Novel Immune-Related Gene Signature for Risk Stratification and Prognosis of Survival in Lower-Grade Glioma. Front Genet 2020; 11: 363.
40) Xiao Y, Zhu Z, Li J, Yao J, Jiang H, Ran R, Li X, Li Z. Expression and prognostic value of long non-coding RNA H19 in glioma via integrated bioinformatics analyses. Aging (Albany NY) 2020; 12: 3407-3430.
41) Liu DH, Wang SL, Hua Y, Shi GD, Qiao JH, Wei H. Five lncRNAs associated with the survival of hepatocellular carcinoma: a comprehensive study based on WGCNA and competing endogenous RNA network. Eur Rev Med Pharmacol Sci 2020; 24: 7621-7633.
42) Li W, Gao LN, Song PP, You CG. Development and validation of a RNA binding protein-associated prognostic model for lung adenocarcinoma. Aging (Albany NY) 2020; 12: 3558-3573.
43) Wickham H. Ggplot2: elegant graphics for data analysis. Springer-Verlag New York; 2009.
44) Chen H, Boutros PC. VennDiagram: a package for the generation of highly-customizable Venn and Euler diagrams in R. BMC bioinformatics 2011; 12: 35.
45) Jiang Y, Zhang Q, Hu Y, Li T, Yu J, Zhao L, Ye G, Deng H, Mou T, Cai S, Zhou Z, Liu H, Chen G, Li G, Qi X. ImmunoScore Signature: A Prognostic and Predictive Tool in Gastric Cancer. Ann Surg 2018; 267: 504-513.
46) Bai J, Zhang X, Xiang ZX, Zhong PY, Xiong B. Identification of prognostic immune-related signature predicting the overall survival for colorectal cancer. Eur Rev Med Pharmacol Sci 2020; 24: 1134-1141.

47) Heagerty PJ, Zheng Y. Survival model predictive accuracy and ROC curves. Biometrics. 2005; 61: 92-105.

48) Gu HY, Zhang C, Guo J, Yang M, Zhong HC, Jin W, Liu Y, Gao LP, Wei RX. Risk score based on expression of five novel genes predicts survival in soft tissue sarcoma. Aging (Albany NY) 2020; 12: 3807-3827.

49) Thul PJ, Åkesson L, Wiking M, Mahdessian D, Geladaki A, Ait Blal H, Alm T, Asplund A, Björk L, Breckels LM, Bäckström A, Danielsson F, Fagerberg L, Fall J, Gatto L, Gnann C, Hober S, Hjelmare M, Johansson F, Lee S, Lindskog C, Mulder J, Mulvey CM, Nilsson P, Oksvold P, Rockberg J, Schutten R, Schwenk JM, Sivertsson Å, Sjöstedt E, Skogs M, Stadler C, Sullivan DP, Tegel H, Winsnes C, Zhang C, Zwahlen M, Mardinoglu A, Pontén F, von Feilitzen K, Lilley KS, Uhlén M, Lundberg E. A subcellular map of the human proteome. Science 2017; 356.

50) Sun Y, Dai WR, Xia N. Comprehensive analysis of lncRNA-mediated ceRNA network in papillary thyroid cancer. Eur Rev Med Pharmacol Sci 2020; 24: 10003-10014.

51) Huang da W, Sherman BT, Lempicki RA. Systematic and integrative analysis of large gene lists using DAVID bioinformatics resources. Nat Protoc 2009; 4: 44-57.

52) Liu JH, Xu YM, Yan J. An 11-lncRNA risk scoring model predicts prognosis of lung squamous cell carcinoma. Eur Rev Med Pharmacol Sci 2020; 24: 5456-5464.

53) Wang LX, Li Y, Chen GZ. Network-based co-expression analysis for exploring the potential diagnostic biomarkers of metastatic melanoma. PLoS One 2018; 13: e0190447.

54) Viappiani S, Nicolescu AC, Holt A, Sawicki G, Crawford BD, León H, van Mulligen T, Schulz R. Activation and modulation of 72kDa matrix metalloproteinase-2 by peroxynitrite and glutathione. Biochem Pharmacol 2009; 77: 826-834.

55) Rotte A, Martinka M, Li G. MMP2 expression is a prognostic marker for primary melanoma patients. Cell Oncol (Dordr) 2012; 35: 207-216.

56) Väisänen AH, Kallioinen M, Turpeenniemi-Hujanen T. Comparison of the prognostic value of matrix metalloproteinases 2 and 9 in cutaneous melanoma. Hum Pathol 2008; 39: 377-385.

57) Hofmann UB, Houben R, Bröcker E-B, Becker JC. Role of matrix metalloproteinases in melanoma cell invasion. Biochimie 2005; 87: 307-314.

58) Singh B, Schneider M, Knyazev P, Ullrich A. UV-induced EGFR signal transactivation is dependent on proligand shedding by activated metalloproteases in skin cancer cell lines. Int J Cancer 2009; 124: 531-539.

59) Kataoka H. EGFR ligands and their signaling scissors, ADAMs, as new molecular targets for anticancer treatments. J Dermatol Sci 2009; 56: 148-153.

60) Bracalente C, Ibañez IL, Berenstein A, Notcovich C, Cerda MB, Klamt F, Chernomoretz A, Durán H. Reprogramming human A375 amelanotic melanoma cells by catalase overexpression: Upregulation of antioxidant genes correlates with regression of melanoma malignancy and with malignant progression when downregulated. Oncotarget 2016; 7: 41154-41171.

61) Erb P, Ji J, Kump E, Mielgo A, Wernli M. Apoptosis and pathogenesis of melanoma and nonmelanoma skin cancer. Adv Exp Med Biol 2008; 624: 283-295.

62) Zhu J, Lin FH, Zhang J, Lin J, Li H, Li YW, Tan XW, Tan JH. The signaling pathways by which the Fas/FasL system accelerates oocyte aging. Aging (Albany NY) 2016; 8: 291-303.

63) Bhardwaj A, Aggarwal BB. Receptor-mediated choreography of life and death. J Clin Immunol 2003; 23: 317-332.

64) Helmbach H, Rossmann E, Kern MA, Schadendorf D. Drug-resistance in human melanoma. Int J Cancer 2001; 93: 617-622.

65) Reuter S, Gupta SC, Chaturvedi MM, Aggarwal BB. Oxidative stress, inflammation, and cancer: how are they linked? Free Radic Biol Med 2010; 49: 1603-1616.

66) Hecht F, Pessoa CF, Gentile LB, Rosenthal D, Carvalho DP, Fortunato RS. The role of oxidative stress on breast cancer development and therapy. Tumour Biol 2016; 37: 4281-4291.

67) Yan X, Wan H, Hao X, Lan T, Li W, Xu L, Yuan K, Wu H. Importance of gene expression signatures in pancreatic cancer prognosis and the establishment of a prediction model. Cancer Manag Res 2019; 11: 273-283.